

Witnessing quantum resource conversion within deterministic quantum computation using one pure superconducting qubit

W. Wang,¹ B. Yadin,² Y. Ma,¹ J. Ma,¹ Y. Xu,¹ L. Hu,¹ H. Wang,¹ Y. P. Song,¹ Mile Gu,^{3,4,5,*} and L. Sun^{1,†}

¹Center for Quantum Information, Institute for Interdisciplinary Information Sciences, Tsinghua University, Beijing 100084, China

²Atomic and Laser Physics, Clarendon Laboratory, University of Oxford, Parks Road, Oxford, OX1 3PU, United Kingdom

³School of Physical and Mathematical Sciences, Nanyang Technological University, Singapore 639673, Republic of Singapore

⁴Complexity Institute, Nanyang Technological University, Singapore 639673, Republic of Singapore

⁵Centre for Quantum Technologies, National University of Singapore,

3 Science Drive 2, Singapore 117543, Republic of Singapore

Deterministic quantum computation with one qubit (DQC1) is iconic in highlighting that exponential quantum speedup may be achieved with negligible entanglement. Its discovery catalyzed heated study of general quantum resources, and various conjectures regarding their role in DQC1's performance advantage. Coherence and discord are prominent candidates, respectively characterizing non-classicality within localized and correlated systems. Here we realize DQC1 within a superconducting system, engineered such that the dynamics of coherence and discord can be tracked throughout its execution. We experimentally confirm that DQC1 acts as a resource converter, consuming coherence to generate discord during its operation. Our results highlight superconducting circuits as a promising platform for both realizing DQC1 and related algorithms, and experimentally characterizing resource dynamics within quantum protocols.

Quantum technologies promise to deliver advantages in wide range of information processing tasks from secure communication [1, 2], solving classically intractable problems [3, 4] to the simulation of complex systems [5–7]. The conventional view held that entanglement enabled this quantum advantage, a quantum resource that plays pivotal roles in many quantum-enhanced protocols [8]. However, this picture is incomplete. The deterministic quantum computation with one qubit (DQC1) model of computation provides a noteworthy counterpoint [9]. The protocol enables exponential quantum speedup in evaluating the normalized trace of unitary matrices, and yet contains little or no entanglement [10, 11]. This motivated a heated search for alternative explanations regarding its source of quantum advantage [12], and catalyzed the recognition that non-classicality comes in many forms.

Iconic among such developments was discord [13], capturing a more robust form of correlations that can persist in environments where entanglement vanishes. Quantum resources were also proposed to describe non-classical properties to individual systems. This resulted in a framework for quantifying non-classicality within coherent quantum superpositions [14] that has since undergone extensive study [15–30]. Meanwhile, different resources were shown to be convertible into each other, a key example being the use of coherence as a resource for generating quantum correlations [21–23, 31]. The manipulation and interplay of these resources is considered a crucial element for understanding the origin of the power of quantum protocols. Indeed, current propositions of how DQC1 gains its operation power include the build-up of discord [12] and, more recently, the conversion of coherence to quantum correlations [22].

Here we realize the DQC1 algorithm within a superconducting system with a circuit quantum electrodynamics (QED) architecture [32–34], and monitor the interplay between coherence and discord in the DQC1 model. We implement the algorithm by coherent control and quantum non-

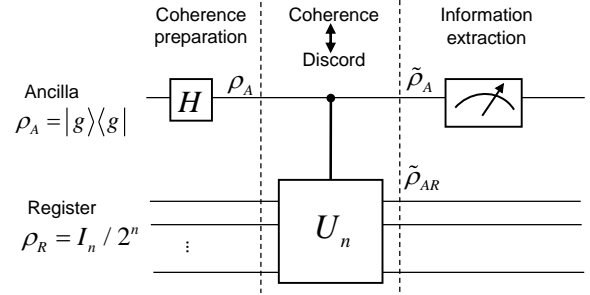


FIG. 1. **DQC1 model.** Initially the ancilla qubit is prepared in a pure ground state and the register qubits are prepared in a maximally mixed state. Coherence in the quantum system is then prepared in the ancilla qubit by a Hadamard gate and converted into discord by a controlled operation U_n . Measurements of $\langle \sigma_x \rangle$ and $\langle \sigma_y \rangle$ on the ancilla qubit give the real and imaginary parts of $\text{Tr}(U_n)/2^n$ respectively.

demolition (QND) projective measurements on a single pure superconducting qubit dispersively coupled to a harmonic oscillator that can potentially provide a maximally mixed state with arbitrary dimension. In particular, we perform full joint state tomography on the combined system to characterize the behavior of coherence and discord in the algorithm. Even in the presence of experimental imperfections, we verify that, as theoretically predicted in Ref. 22, the amount of discord generated during the computation is upper bounded by the consumption of the initial coherence of the system. Our work provides the first experimental characterization of resource conversion dynamics within DQC1, and extends previous experimental realizations of DQC1 in linear optics [35] and liquid-state nuclear magnetic resonance [36] to a new technological medium.

We first review theoretical preliminaries. Coherence is taken here to mean the superposition of states in some preferred basis set $\{|i\rangle\}$. There is often a natural physical basis

to consider – here, it will be the energy basis of the superconducting qubit. The resource theory of coherence [14] provides criteria for determining valid measures of coherence. One first defines the set of states with no coherence \mathcal{I} , or incoherent states, to be all states of the form $\sigma = \sum_i p_i |i\rangle\langle i|$. A good coherence measure must vanish exactly on this set. Next, one defines incoherent operations to be those quantum operations having a set of Kraus operators $\{K_i\}$ with the property $K_i \mathcal{I} K_i^\dagger \in \mathcal{I}$. This condition says that an incoherent operation is never able to create coherence from an incoherent state. The next criterion for a valid coherence measure is then that it cannot increase under an incoherent operation. A number of interesting measures satisfying these criteria have been found [37]. We use the relative entropy of coherence [14], defined as

$$C(\rho) := \min_{\sigma \in \mathcal{I}} S(\rho || \sigma) \quad (1)$$

$$= S(\rho^{diag}) - S(\rho), \quad (2)$$

where $S(\rho) = -\text{Tr} \rho \log \rho$ is the von Neumann entropy, $S(\rho || \sigma) = -S(\rho) - \text{Tr} \rho \log \sigma$ is the relative entropy, and ρ^{diag} is the state obtained by removing the off-diagonal elements of ρ in the reference basis $\{|i\rangle\}$.

Quantum discord has a number of characterizations, the first historically being the gap between the total correlations and the classical correlations accessible from local measurements [38, 39]. In a system partitioned into n subsystems $\{A_1, A_2, \dots, A_n\}$, states with vanishing discord are called classically correlated. They take the form $\sum_{k_1, \dots, k_n} p_{k_1, \dots, k_n} |k_1, \dots, k_n\rangle\langle k_1, \dots, k_n|$, where $\{p_{k_1, \dots, k_n}\} \geq 0$, $\sum_{k_1, \dots, k_n} p_{k_1, \dots, k_n} = 1$ and $\{|k_1, \dots, k_n\rangle\} = |k_1\rangle \otimes \dots \otimes |k_n\rangle$ is an arbitrary product basis. Classically correlated states are separable (not entangled), but not every separable state is classically correlated. There are many proposed measures of discord [13, 40]; we focus on one measure which treats all subsystems equally, named global discord [41]. This is defined by

$$D(\rho_{A_1, \dots, A_n}) = \min_{\Phi^i} S(\rho_{A_1, \dots, A_n} || \Phi^i(\rho_{A_1, \dots, A_n})) - \sum_k S(\rho_{A_k} || \Phi_{A_k}^i(\rho_{A_k})) \quad (3)$$

where $\Phi^i = \otimes_{j=1}^n \Phi_{A_j}^i$, $\Phi_{A_k}^i(\rho_{A_k}) = \sum_i |i_k\rangle\langle i_k| \rho_{A_k} |i_k\rangle\langle i_k|$ is the dephasing operation, and the minimization is over all dephasing basis choices.

The DQC1 protocol is illustrated in Fig. 1. The quantum circuit is fed with $n + 1$ qubits, consisting of one pure ancilla qubit and n maximally mixed register qubits. As noted in Ref. 22, coherence-to-discord conversion takes place in this algorithm. Specifically, coherence is initially generated in the ancilla qubit by a Hadamard gate. Then a controlled- U gate is performed to correlate the ancilla and the register qubits, and thus create discord between the ancilla and register qubits at the cost of the coherence in the ancilla qubit. Note that the reference basis for defining coherence is taken to coincide with the control basis of this gate. This process is encapsulated in

the following inequality:

$$D(\tilde{\rho}_{AR}) \leq \Delta C(\rho_A), \quad (4)$$

where $\tilde{\rho}_{AR}$ is the joint state of the $n + 1$ qubits after the controlled- U gate, $\Delta C(\rho_A) = C(\rho_A) - C(\tilde{\rho}_A)$ is the coherence consumption during the controlled- U gate, with ρ_A and $\tilde{\rho}_A$ the states of the ancilla qubit before and after the controlled- U gate, respectively.

We realize the DQC1 algorithm using a superconducting transmon qubit dispersively coupled to two waveguide cavity resonators [33, 42–45], as shown in Fig. 2a. The transmon qubit has a fixed frequency of $\omega_a/2\pi = 5.295$ GHz, an energy relaxation time $T_1 = 12 \mu\text{s}$, and a pure dephasing time $T_\phi = 14 \mu\text{s}$. One of the cavities (storage cavity) has a long photon lifetime of $\tau_s = 80 \mu\text{s}$ with a resonant frequency $\omega_s/2\pi = 8.33$ GHz. The Fock states in this storage cavity (composing the register qubits) and the transmon qubit (as the ancilla) constitute the bipartite parts of the DQC1 circuit [13]. The other short-lived cavity with a photon lifetime $\tau_r = 40$ ns and a frequency $\omega_r/2\pi = 7.29$ GHz is used to readout the ancilla qubit. The qubit readout is performed by a homodyne detection of the qubit state-dependent cavity response [46] with the help of a phase-sensitive Josephson bifurcation amplification [47–50] for a high fidelity and QND single-shot measurement. Each readout measurement throughout our experiment returns a digitized value of the qubit state. The experimental apparatus and readout properties are similar to earlier reports in Refs. 45 and 51. The ancilla qubit and storage cavity are well described by the dispersive Hamiltonian (omitting small high-order nonlinearities)

$$H/\hbar = \omega_s a^\dagger a + \omega_a |e\rangle\langle e| - \chi a^\dagger a |e\rangle\langle e| \quad (5)$$

where a^\dagger (a) is the creation (annihilation) operator of the storage cavity, $|e\rangle$ is the excited state of the ancilla qubit, and $\chi/2\pi = 1.34$ MHz is the dispersive interaction strength between the qubit and the storage cavity. This strong dispersive coupling gives rise to the ancilla-register entangling operation, allowing for the controlled- U operation in the DQC1 algorithm. The readout cavity has been neglected since it remains in vacuum unless a measurement is performed.

Harmonic oscillators play important roles in quantum information processing [52–55] largely due to their infinite dimension and long coherence times. Here we take advantage of these characteristics to use multiple excitations of a harmonic cavity oscillator as register qubit states. In our experiment, we choose the lowest four Fock states $|0\rangle, |1\rangle, |2\rangle$, and $|3\rangle$ in the cavity field whose computational space is equivalent to that of two register qubits, namely $|00\rangle, |01\rangle, |10\rangle$, and $|11\rangle$ respectively. This gives the DQC1 model in our experiment with $n = 2$ register qubits. Considering the infinite dimension of the cavity resonator, one could in principle achieve an arbitrarily large DQC1 system.

Our experimental sequence is depicted in Fig. 2b. The whole process can be divided into three parts: state preparation, DQC1 algorithm, and joint tomography measurement.

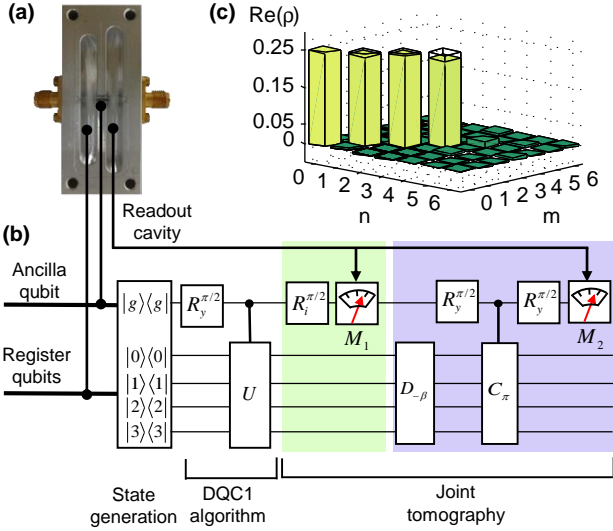


FIG. 2. **Experimental quantum circuit to measure the conversion between coherence and quantum correlations with a DQC1 model.** (a) Optical image of a transmon qubit, as an ancilla qubit, dispersively coupled to two waveguide cavities. The lowest four Fock states in the storage cavity are designated as the register qubit states. (b) The whole process can be divided into three parts: state preparation, DQC1 algorithm, and joint tomography measurement. A $\pi/2$ rotation along the y -axis $R_y^{\pi/2}$, corresponding to a Hadamard gate on the ancilla qubit, creates input coherence in this circuit. The register states evolve different phase shifts dependent on the ancilla state (a controlled- U gate). To overcome the difficulty of generating a maximally mixed state of the register qubit, we prepare the register qubit in a pure Fock state $|k\rangle$ ($k=0, 1, 2, 3$) one at a time, run the whole sequence separately, and finally mix the experimental results with equal weight. Those Fock states are generated separately by the Gradient Ascent Pulse Engineering method [56, 57] with fidelities of 0.951, 0.936, 0.929, and 0.924 respectively, based on the corresponding Wigner function. Joint tomography is performed by correlating the ancilla qubit tomography and subsequent register qubits Wigner tomography (see details in the main text). To make each initial ancilla-register state $(|g\rangle\langle g| \otimes |k\rangle\langle k|)$ undergo identical DQC1 operations, the first $R_y^{\pi/2}$ for coherence preparation and the pre-rotation pulses $R_i^{\pi/2}$ for the ancilla qubit tomography are all driven at the qubit frequency corresponding to each $|k\rangle$. The phase φ in the controlled- U gate is realized through a suitable phase adjustment in the pre-rotation pulses $R_i^{\pi/2}$. (c) Real part of the reconstructed density matrix (truncated to maximum photon number state $N_{max} = 6$) of the initial register qubits through an average of the separate Wigner tomography of each $|k\rangle$ ($k=0, 1, 2, 3$) state.

The state preparation starts with a pure qubit ground state $|g\rangle\langle g|$ by post-selection, however, it is not straightforward in our experiment to generate a maximally mixed state as required by the DQC1 model. For simplicity, we instead initialize the register qubit state to a pure Fock state $|k\rangle$ ($k=0, 1, 2, 3$) in the cavity field one at a time, run the whole sequence separately, and finally mix the experimental results with equal weight. Note that the register qubits do not contribute any coherence to the combined system.

In the following DQC1 algorithm, coherence preparation is

performed by an ancilla qubit operation $R_y^{\pi/2}$ corresponding to a $\pi/2$ rotation around the y -axis on the Bloch sphere, having the same action here as a Hadamard gate. Consequently, the system is prepared in a product state $|\psi_k\rangle = (|g\rangle + |e\rangle) \otimes |k\rangle$ (ignoring normalization). A conditional cavity phase shift $C_\varphi = \mathbf{1} \otimes |g\rangle\langle g| + e^{i\varphi a^\dagger a} \otimes |e\rangle\langle e|$ is the mechanism of the controlled- U gate, where $\varphi = \chi t$ is acquired from the free evolution of the dispersive Hamiltonian Eq. 5 for a time interval t . As a result, the controlled- U gate can be described as $\mathbf{1} \otimes |g\rangle\langle g| + U \otimes |e\rangle\langle e|$, where

$$U = \begin{pmatrix} 1 & 0 & 0 & 0 \\ 0 & e^{i\varphi} & 0 & 0 \\ 0 & 0 & e^{2i\varphi} & 0 \\ 0 & 0 & 0 & e^{3i\varphi} \end{pmatrix} \quad (6)$$

in the computational Hilbert space. Note that in the Fock state basis, the controlled- U is an incoherent operation. After the controlled- U gate, the system evolves to $|\tilde{\psi}_k\rangle = (|g\rangle + e^{ik\varphi}|e\rangle) \otimes |k\rangle$.

To observe the bipartite system, we finally perform a joint measurement of the coupled ancilla-register system with two sequential QND measurements of the ancilla qubit and the register qubits, following a technique similar to that previously demonstrated in Ref. 58. As shown in Fig. 2b, the ancilla qubit detections along one of the three basis vectors X, Y , and Z are first performed with or without an appropriate pre-rotation $R_i^{\pi/2}$ followed by a z -basis measurement M_1 . These measurements alone can give a full tomography of the ancilla. Then a Wigner tomography of the register qubit is performed by measuring the cavity observable $P(\beta)$ which is a combination of the cavity's displacement operation $D_{-\beta}$ and a parity measurement P of the cavity. The parity measurement is realized in a Ramsey-type experiment of the ancilla qubit, where a conditional cavity π phase shift C_π is sandwiched in between two unconditional qubit rotations $R_y^{\pi/2}$ followed by another z -basis measurement M_2 [43, 44, 59, 60]. After the qubit tomography measurement M_1 the qubit is at a specific known state and the correlation of M_1 and M_2 determines the parity of the register. Multiplication of the ancilla qubit detection σ_i (in the qubit Pauli set $\{I, X, Y, Z\}$) and the register Wigner tomography $W_k(\beta)$ (the subscript k denotes the register initial state at $|k\rangle$) shot-by-shot gives the joint Wigner function [58], defined as:

$$W_{ik}(\beta) = \frac{2}{\pi} \langle \sigma_i P_k(\beta) \rangle \quad (7)$$

For any specific phase φ in the controlled- U gate, as mentioned above, we generate the initial register qubit state $|k=0, 1, 2, 3\rangle$ one at a time and follow exactly the same circuit in Fig. 2b individually. Since the Wigner function is linear, this allows to acquire the joint Wigner functions W_i for the case of a mixed initial register state by averaging the four joint Wigner functions W_{ik} corresponding to a pure Fock state

$|k\rangle$ as the initial register state. Explicitly, we have:

$$W_i(\beta) = \frac{1}{4} \sum_{k=0}^3 W_{ik}(\beta) \quad (8)$$

These four joint Wigner functions are a complete representation of the combined ancilla-register quantum system. From these functions we reconstruct the combined ancilla-register density matrix $\tilde{\rho}_{AR}$ in an eight-dimensional Hilbert space by a least squares regression using maximum likelihood estimation with the only constraints that the reconstructed density matrix is positive semi-definite with trace equal to one [58, 61]. Based on the obtained density matrix $\tilde{\rho}_{AR}$, we can derive the remaining coherence $C(\tilde{\rho}_A)$ and the created discord $D(\tilde{\rho}_{AR})$ according to Eqs. 2 and 3, where $\tilde{\rho}_A$ is the partial trace of $\tilde{\rho}_{AR}$ over the registers.

The initial coherence is generated by the ancilla qubit operation $R_y^{\pi/2}$ and is first characterized to be $C(\rho_A) = 0.95$ by a qubit tomography immediately after this coherent operation (Fig. 2b). The reduction is mainly due to a qubit decay process during the tomography measurement. This initial coherence built in the ancilla state is then to be consumed in order to correlate the ancilla and the register qubits, and thus is used as a reference for the coherence consumption. We next show the results after applying the controlled- U gate in the DQC1 model. The normalized trace of U is encoded in the ancilla qubit and can be recovered from the result of M_1 , as shown in Fig. 3. Although there are decoherence processes with both ancilla and register qubits, the experimental results (dots) agree well with the exact theoretical expectation (lines) and the numerical simulation (crosses) that involves all imperfection channels, suggesting the robustness of the protocol.

We finally show in Fig. 4 the coherence consumption $\Delta C(\rho_A)$ and discord production $D(\tilde{\rho}_{AR})$ in the DQC1 model as a function of phase φ in the controlled- U gate which varies over the range $0 \leq \varphi \leq 2\pi$ with a step of $\pi/8$. Theoretical expectations of $\Delta C(\rho_A)$ and $D(\tilde{\rho}_{AR})$ for an ideal system without any decoherence are shown as solid lines for comparison. Both curves are symmetric around $\varphi = \pi$. At $\varphi = \pi$, the controlled- U gate is expected to transform the qubit-register system into a classically correlated state without any discord. At $\varphi = \pi/2, \pi, 3\pi/2$, after tracing out the register state the ancilla qubit is in a maximally mixed state. In these cases, the original coherence is completely consumed by the controlled- U operation. The gap between the expected solid lines means that, even theoretically, coherence can not be fully converted to discord. The non-monotonic oscillations in the theoretical curves are not fully understood yet and need further investigation. To characterize these subtle features in theory, especially for $D(\tilde{\rho}_{AR})$, we replace $5\pi/8$ and $11\pi/8$ with 0.653π and 1.343π respectively.

The experimental results for both $\Delta C(\rho_A)$ and $D(\tilde{\rho}_{AR})$ are depicted as dots and are indeed quite symmetric around $\varphi = \pi$, and capture all the important features in the theoretical curves. The measured coherence consumption agrees fairly well with theory except for the first and last data points. The

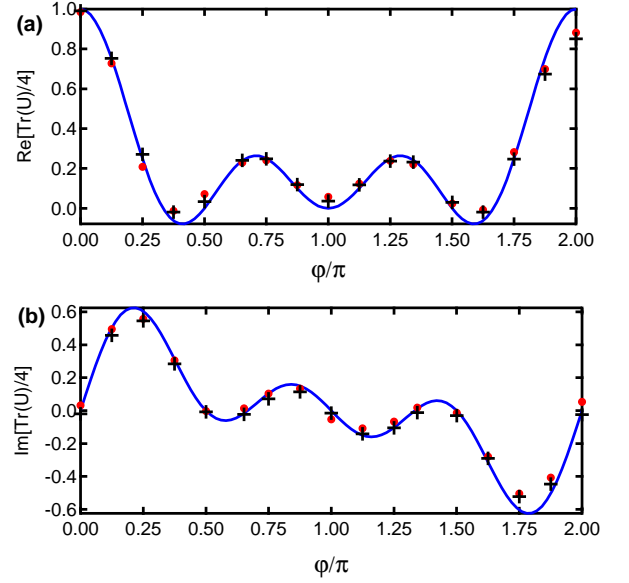


FIG. 3. **DQC1 algorithm output.** The normalized trace of U is encoded in the ancilla qubit and is recovered from the results of M_1 in Fig. 2b. The upper (a) and lower (b) panels are the real and imaginary part of the normalized trace $\text{Tr}(U)/4$ measured for different φ respectively. All data (points) are averaged with about 10^7 measurements and error bars corresponding to one standard deviation are smaller than marker sizes. The solid lines show theoretical expectations. Crosses present the simulated results including all decoherence channels. Experiment results agree well with both theory and simulation even with the presence of decoherence processes from both ancilla and register qubits.

small gap at the middle plateau is consistent with the initial coherence $C_{\rho_A} = 0.95$. The first data point for $\Delta C(\rho_A)$ is much larger than zero and can be attributed to the decoherence and imperfections during the joint Wigner tomography operation. This can be verified by a good match with the numerical simulation (cross) including the system decoherence. For the last point, the deviation from zero is even larger because of the extra decoherence in the long operation time (~ 750 ns) in the controlled- U gate.

However, there is an obvious gap between the measured and theoretical produced discord. This gap comes from the fact that, besides being converted to the discord in the combined system, the initial coherence of the ancilla qubit inevitably decays to the surroundings during the algorithm due to decoherence. This large effect from decoherence has been confirmed by the good match between the measured and simulated $D(\tilde{\rho}_{AR})$. Nevertheless, all measured $D(\tilde{\rho}_{AR})$ are significantly lower than the measured $\Delta C(\rho_A)$, successfully demonstrating Eq. 4. The inset in Fig. 4 shows the state fidelity of the ancilla-register system at each φ based on the measured $\tilde{\rho}_{AR}$. All fidelities are above 0.92, demonstrating the good control of our system throughout the process.

We note that in Eq. 5 the higher order corrections to the dispersive term, such as $(\chi'/2)a^\dagger a^\dagger aa|e\rangle\langle e|$ (χ' is typically more

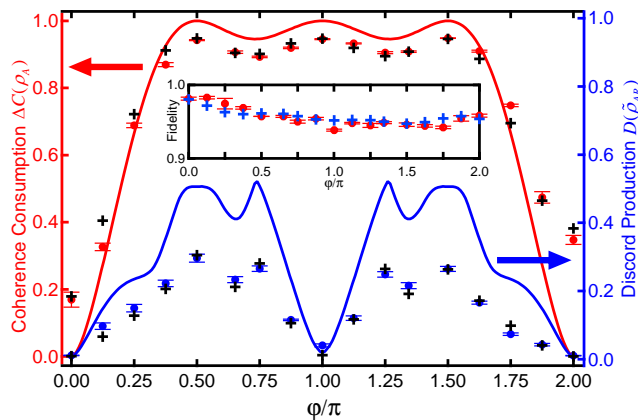


FIG. 4. **The coherence consumption $\Delta C(\rho_A)$ and discord production $D(\tilde{\rho}_{AR})$ as a function of phase ϕ in the DQC1 model.** Theoretical expectations are shown with solid lines. Dots give the experimental results. In the experiment, each point in the joint Wigner functions has been averaged over 1000 single-shot joint ancilla and register measurements, and the standard deviation in $\Delta C(\rho_A)$ and $D(\tilde{\rho}_{AR})$ are estimated by bootstrapping on the measured joint Wigner functions [58]. Crosses present the simulated data including all decoherence channels with both the ancilla and register qubits. The measured $\Delta C(\rho_A)$ agrees fairly well with the theoretical one except for the first and last data points. There is a significant gap between the measured and theoretical $D(\tilde{\rho}_{AR})$. However, the measured $D(\tilde{\rho}_{AR})$ captures all the important features as in the theoretical curve and is unambiguously lower than $\Delta C(\rho_A)$ as expected. The gap comes from the fact that, besides being converted to the discord in the system, the initial coherence of the ancilla qubit inevitably decays to the surroundings during the algorithm process due to decoherence. The inset shows the fidelity of the measured $\tilde{\rho}_{AR}$ compared to the ideal ones. The high fidelities, all above 0.92, demonstrate the good control of the quantum system in the whole process.

than two orders of magnitude smaller than χ), have been ignored because of their small contribution to ϕ compared to the dispersive term in the small photon number limit. However, these higher order non-linear terms in principle allow for generating arbitrary controlled- U by repeated applications of appropriate cavity displacements followed by appropriate waiting, provided the system has enough coherence [62–65].

In conclusion, we have experimentally demonstrated and quantified quantum resource conversion in the DQC1 model. We show that coherence is converted into the quantum discord that is considered as the resource in DQC1 [12]. The produced discord is unambiguously demonstrated to be lower than the coherence consumption. This is accomplished based on a superconducting circuit QED architecture with an intrinsic dispersive coupling between a superconducting transmon qubit and a waveguide cavity. This experiment reveals the potential of superconducting circuits as a versatile platform for investigating and even deepening our understanding of resource dynamics in quantum information.

A natural extension of the present work is to chain multiple DQC1 circuits together. Provided the register qubits are not reset between iterations, the resulting circuit enables a variant of Shor’s algorithm [66, 67]. Here, each iteration

converts an additional bit of coherence into quantum correlations, enabling study of resource conversion dynamics within the iconic quantum factoring protocol. A second variation is “power of one pure qumode” protocol – in which the control qubit in DQC1 is replaced with a continuous variable mode to form a hybrid model of computation that combines discrete and continuous variables [68]. This protocol may be a natural fit for our architecture, where the cavity mode is intrinsically a continuous variable degree of freedom. Its realization could enable hybrid factoring algorithms, and aid the study of how continuous and discrete notions of non-classicality interact. Each of these developments would provide a promising experimental platform for studying quantum resource dynamics within more complex settings.

* mgu@quantumcomplexity.org

† luyansun@tsinghua.edu.cn

- [1] N. Gisin, G. Ribordy, W. Tittel, and H. Zbinden, “Quantum cryptography,” *Rev. Mod. Phys.* **74**, 145 (2002).
- [2] V. Scarani, H. Bechmann-Pasquinucci, N. J. Cerf, M. Dušek, N. Lütkenhaus, and M. Peev, “The security of practical quantum key distribution,” *Rev. Mod. Phys.* **81**, 1301 (2009).
- [3] P. W. Shor, “Algorithms for quantum computation: Discrete logarithms and factoring,” in *Foundations of Computer Science, 1994 Proceedings., 35th Annual Symposium on (IEEE, 1994)* pp. 124–134.
- [4] L. K. Grover, “A fast quantum mechanical algorithm for database search,” in *Proceedings of the twenty-eighth annual ACM symposium on Theory of computing (ACM, 1996)* pp. 212–219.
- [5] S. Lloyd, “Universal quantum simulators,” *Science* **273**, 1073 (1996).
- [6] I. M. Georgescu, S. Ashhab, and F. Nori, “Quantum simulation,” *Reviews of Modern Physics* **86**, 153 (2014).
- [7] M. Gu, K. Wiesner, E. Rieper, and V. Vedral, “Quantum mechanics can reduce the complexity of classical models,” *Nature Communications* **3**:762 (2012), doi:10.1038/ncomms1761.
- [8] R. Horodecki, P. Horodecki, M. Horodecki, and K. Horodecki, “Quantum entanglement,” *Reviews of Modern Physics* **81**, 865 (2009).
- [9] E. Knill and R. Laflamme, “Power of one bit of quantum information,” *Physical Review Letters* **81**, 5672 (1998).
- [10] A. Datta and G. Vidal, “Role of entanglement and correlations in mixed-state quantum computation,” *Phys. Rev. A* **75**, 042310 (2007).
- [11] M. Hor-Meyll, D. S. Tasca, S. P. Walborn, P. H. S. Ribeiro, M. M. Santos, and E. I. Duzzioni, “Deterministic quantum computation with one photonic qubit,” *Phys. Rev. A* **92**, 012337 (2015).
- [12] A. Datta, A. Shaji, and C. M. Caves, “Quantum discord and the power of one qubit,” *Phys. Rev. Lett.* **100**, 050502 (2008).
- [13] K. Modi, A. Brodutch, H. Cable, T. Paterek, and V. Vedral, “The classical-quantum boundary for correlations: Discord and related measures,” *Rev. Mod. Phys.* **84**, 1655 (2012).
- [14] T. Baumgratz, M. Cramer, and M. B. Plenio, “Quantifying coherence,” *Phys. Rev. Lett.* **113**, 140401 (2014).
- [15] D. Girolami, “Observable measure of quantum coherence in finite dimensional systems,” *Phys. Rev. Lett.* **113**, 170401 (2014).

- [16] T. R. Bromley, M. Cianciaruso, and G. Adesso, “Frozen quantum coherence,” *Phys. Rev. Lett.* **114**, 210401 (2015).
- [17] X. Yuan, H. Zhou, Z. Cao, and X. Ma, “Intrinsic randomness as a measure of quantum coherence,” *Phys. Rev. A* **92**, 022124 (2015).
- [18] S. Cheng and M. J. W. Hall, “Complementarity relations for quantum coherence,” *Phys. Rev. A* **92**, 042101 (2015).
- [19] Y. Yao, X. Xiao, L. Ge, and C. P. Sun, “Quantum coherence in multipartite systems,” *Phys. Rev. A* **92**, 022112 (2015).
- [20] L.-H. Shao, Z. Xi, H. Fan, and Y. Li, “Fidelity and trace-norm distances for quantifying coherence,” *Phys. Rev. A* **91**, 042120 (2015).
- [21] A. Streltsov, U. Singh, H. S. Dhar, M. N. Bera, and G. Adesso, “Measuring quantum coherence with entanglement,” *Physical Review Letters* **115**, 020403 (2015).
- [22] J. Ma, B. Yadin, D. Girolami, V. Vedral, and M. Gu, “Converting coherence to quantum correlations,” *Physical Review Letters* **116**, 160407 (2016).
- [23] E. Chitambar, A. Streltsov, S. Rana, M. Bera, G. Adesso, and M. Lewenstein, “Assisted distillation of quantum coherence,” *Physical Review Letters* **116**, 070402 (2016).
- [24] A. Winter and D. Yang, “Operational resource theory of coherence,” *Phys. Rev. Lett.* **116**, 120404 (2016).
- [25] C. Napoli, T. R. Bromley, M. Cianciaruso, M. Piani, N. Johnston, and G. Adesso, “Robustness of coherence: An operational and observable measure of quantum coherence,” *Phys. Rev. Lett.* **116**, 150502 (2016).
- [26] B. Yadin, J. Ma, D. Girolami, M. Gu, and V. Vedral, “Quantum processes which do not use coherence,” *Phys. Rev. X* **6**, 041028 (2016).
- [27] S. Rana, P. Parashar, and M. Lewenstein, “Trace-distance measure of coherence,” *Phys. Rev. A* **93**, 012110 (2016).
- [28] X. Yuan, K. Liu, Y. Xu, W. Wang, Y. Ma, F. Zhang, Z. Yan, R. Vijay, L. Sun, and X. Ma, “Experimental quantum randomness processing using superconducting qubits,” *Physical Review Letters* **117**, 010502 (2016).
- [29] C. Radhakrishnan, M. Parthasarathy, S. Jambulingam, and T. Byrnes, “Distribution of quantum coherence in multipartite systems,” *Phys. Rev. Lett.* **116**, 150504 (2016).
- [30] J. P. Santos, L. C. Céleri, G. T. Landi, and M. Paternostro, “The role of quantum coherence in non-equilibrium entropy production,” arXiv:1707.08946 (2017).
- [31] K. Wu, Z. Hou, Y. Zhao, G. Xiang, C. Li, G. Guo, J. Ma, Q. He, J. Thompson, and M. Gu, “Experimental cyclic inter-conversion between coherence and quantum correlations,” arXiv:1710.01738 (2017).
- [32] A. Wallraff, D. I. Schuster, A. Blais, L. Frunzio, R.-S. Huang, J. Majer, S. Kumar, S. M. Girvin, and R. J. Schoelkopf, “Circuit quantum electrodynamics: Coherent coupling of a single photon to a cooper pair box,” *Nature* **431**, 162 (2004).
- [33] H. Paik, D. I. Schuster, L. S. Bishop, G. Kirchmair, G. Catelani, A. P. Sears, B. R. Johnson, M. J. Reagor, L. Frunzio, L. I. Glazman, S. M. Girvin, M. H. Devoret, and R. J. Schoelkopf, “Observation of high coherence in josephson junction qubits measured in a three-dimensional circuit qed architecture,” *Phys. Rev. Lett.* **107**, 240501 (2011).
- [34] M. H. Devoret and R. J. Schoelkopf, “Superconducting circuits for quantum information: An outlook,” *Science* **339**, 1169 (2013).
- [35] B. P. Lanyon, M. Barbieri, M. P. Almeida, and A. G. White, “Experimental quantum computing without entanglement,” *Phys. Rev. Lett.* **101**, 200501 (2008).
- [36] G. Passante, O. Moussa, D. A. Trottier, and R. Laflamme, “Experimental detection of nonclassical correlations in mixed-state quantum computation,” *Phys. Rev. A* **84**, 044302 (2011).
- [37] A. Streltsov, G. Adesso, and M. B. Plenio, “Colloquium : Quantum coherence as a resource,” *Reviews of Modern Physics* **89**, 041003 (2017).
- [38] L. Henderson and V. Vedral, “Classical, quantum and total correlations,” *Journal of physics A: mathematical and general* **34**, 6899 (2001).
- [39] H. Ollivier and W. H. Zurek, “Quantum discord: a measure of the quantumness of correlations,” *Physical Review Letters* **88**, 017901 (2001).
- [40] G. Adesso, T. R. Bromley, and M. Cianciaruso, “Measures and applications of quantum correlations,” *Journal of Physics A: Mathematical and Theoretical* **49**, 473001 (2016).
- [41] C. Rulli and M. Sarandy, “Global quantum discord in multipartite systems,” *Physical Review A* **84**, 042109 (2011).
- [42] G. Kirchmair, B. Vlastakis, Z. Leghtas, S. E. Nigg, H. Paik, E. Ginossar, M. Mirrahimi, L. Frunzio, S. M. Girvin, and R. J. Schoelkopf, “Observation of quantum state collapse and revival due to the single-photon Kerr effect,” *Nature* **495**, 205 (2013).
- [43] B. Vlastakis, G. Kirchmair, Z. Leghtas, S. E. Nigg, L. Frunzio, S. M. Girvin, M. Mirrahimi, M. H. Devoret, and R. J. Schoelkopf, “Deterministically encoding quantum information using 100-photon Schrödinger cat states,” *Science* **342**, 607 (2013).
- [44] L. Sun, A. Petrenko, Z. Leghtas, B. Vlastakis, G. Kirchmair, K. M. Sliwa, A. Narla, M. Hatridge, S. Shankar, J. Blumoff, L. Frunzio, M. Mirrahimi, M. H. Devoret, and R. J. Schoelkopf, “Tracking photon jumps with repeated quantum non-demolition parity measurements,” *Nature* **511**, 444 (2014).
- [45] K. Liu, Y. Xu, W. Wang, S.-B. Zheng, T. Roy, S. Kundu, M. Chand, A. Ranadive, R. Vijay, Y. Song, *et al.*, “A twofold quantum delayed-choice experiment in a superconducting circuit,” *Science Advances* **3**, e1603159 (2017).
- [46] A. Blais, R.-S. Huang, A. Wallraff, S. M. Girvin, and R. J. Schoelkopf, “Cavity quantum electrodynamics for superconducting electrical circuits: An architecture for quantum computation,” *Phys. Rev. A* **69**, 062320 (2004).
- [47] M. Hatridge, R. Vijay, D. H. Slichter, J. Clarke, and I. Siddiqi, “Dispersive magnetometry with a quantum limited SQUID parametric amplifier,” *Phys. Rev. B* **83**, 134501 (2011).
- [48] T. Roy, S. Kundu, M. Chand, A. M. Vaddiraj, A. Ranadive, N. Nehra, M. P. Patankar, J. Aumentado, A. A. Clerk, and R. Vijay, “Broadband parametric amplification with impedance engineering: Beyond the gain-bandwidth product,” *Appl. Phys. Lett.* **107**, 262601 (2015).
- [49] A. Kamal, A. Marblestone, and M. H. Devoret, “Signal-to-pump back action and self-oscillation in double-pump Josephson parametric amplifier,” *Phys. Rev. B* **79**, 184301 (2009).
- [50] K. W. Murch, S. J. Weber, C. Macklin, and I. Siddiqi, “Observing single quantum trajectories of a superconducting quantum bit,” *Nature* **502**, 211 (2013).
- [51] W. Wang, L. Hu, Y. Xu, K. Liu, Y. Ma, S.-B. Zheng, R. Vijay, Y. P. Song, L.-M. Duan, and L. Sun, “Converting quasiclassical states into arbitrary fock state superpositions in a superconducting circuit,” *Phys. Rev. Lett.* **118**, 223604 (2017).
- [52] V. Bužek and P. L. Knight, “not sure,” *Progress in Optics* **34**, 1 (1995).
- [53] Z. Leghtas, G. Kirchmair, B. Vlastakis, R. J. Schoelkopf, M. H. Devoret, and M. Mirrahimi, “Hardware-efficient autonomous quantum error correction,” *Phys. Rev. Lett.* **111**, 120501 (2013).
- [54] N. Ofek, A. Petrenko, R. Heeres, P. Reinhold, Z. Leghtas, B. Vlastakis, Y. Liu, L. Frunzio, S. M. Girvin, L. Jiang, M. Mirrahimi, M. H. Devoret, and R. J. Schoelkopf, “Extending the lifetime of a quantum bit with error correction in superconduct-

- ing circuits,” *Nature* **536**, 441 (2016).
- [55] M. H. Michael, M. Silveri, R. T. Brierley, V. V. Albert, J. Salmilehto, L. Jiang, and S. M. Girvin, “New class of quantum error-correcting codes for a bosonic mode,” *Phys. Rev. X* **6**, 031006 (2016).
- [56] N. Khaneja, T. Reiss, C. Kehlet, T. Schulte-Herbrüggen, and S. J. Glaser, “Optimal control of coupled spin dynamics: design of {NMR} pulse sequences by gradient ascent algorithms,” *Journal of Magnetic Resonance* **172**, 296 (2005).
- [57] P. de Fouquieres, S. Schirmer, S. Glaser, and I. Kuprov, “Second order gradient ascent pulse engineering,” *Journal of Magnetic Resonance* **212**, 412 (2011).
- [58] B. Vlastakis, A. Petrenko, N. Ofek, L. Sun, Z. Leghtas, K. Sliwa, Y. Liu, M. Hatridge, J. Blumoff, L. Frunzio, M. Mirrahimi, L. Jiang, M. H. Devoret, and R. J. Schoelkopf, “Characterizing entanglement of an artificial atom and a cavity cat state with bell’s inequality,” *Nature Communications* **6**:8970 (2015).
- [59] L. G. Lutterbach and L. Davidovich, “Method for direct measurement of the wigner function in cavity qed and ion traps,” *Phys. Rev. Lett.* **78**, 2547 (1997).
- [60] P. Bertet, A. Auffeves, P. Maioli, S. Osnaghi, T. Meunier, M. Brune, J. M. Raimond, and S. Haroche, “Direct measurement of the wigner function of a one-photon fock state in a cavity,” *Phys. Rev. Lett.* **89**, 200402 (2002).
- [61] J. A. Smolin, J. M. Gambetta, and G. Smith, “Efficient method for computing the maximum-likelihood quantum state from measurements with additive gaussian noise,” *Phys. Rev. Lett.* **108**, 070502 (2012).
- [62] D. Deutsch, A. Barenco, and A. Ekert, “Universality in quantum computation,” *Proc. R. Soc. London, Ser. A* **449**, 669 (1995).
- [63] S. Lloyd, “Almost any quantum logic gate is universal,” *Phys. Rev. Lett.* **75**, 346 (1995).
- [64] S. L. Braunstein and P. van Loock, “Quantum information with continuous variables,” *Rev. Mod. Phys.* **77**, 513 (2005).
- [65] C.-L. Zou, L. Jiang, X.-B. Zou, and G.-C. Guo, “Filtration and extraction of quantum states from classical inputs,” *Phys. Rev. A* **94**, 013841 (2016).
- [66] S. Parker and M. B. Plenio, “Efficient factorization with a single pure qubit and $\log N$ mixed qubits,” *Phys. Rev. Lett.* **85**, 3049 (2000).
- [67] E. Martín-López, A. Laing, T. Lawson, R. Alvarez, X.-Q. Zhou, and J. L. O’Brien, “Experimental realization of shor’s quantum factoring algorithm using qubit recycling,” *Nature Photonics* **6**, 773 (2012).
- [68] N. Liu, J. Thompson, C. Weedbrook, S. Lloyd, V. Vedral, M. Gu, and K. Modi, “Power of one qumode for quantum computation,” *Phys. Rev. A* **93**, 052304 (2016).

Acknowledgments

We acknowledge Changling Zou for helpful discussions, and thank R. Vijay and his group for help on the parametric amplifier measurements. This work is supported by the National Natural Science Foundation of China under Grant No. 11474177, National Key Research and Development Program of China No. 2017YFA0304303, the 1000 Youth Fellowship program in China, the National Research Foundation of Singapore (Fellowship NRF-NRFF2016-02 and NRF2017-NRFANR004 VanQuTe), and the Singapore Ministry of Education Tier 1 RG190/17.